European Journal of Medicinal Chemistry 248 (2023) 115069

Contents lists available at ScienceDirect

European Journal of Medicinal Chemistry

journal homepage: www.elsevier.com/locate/ejmech

Research paper

Pleiotropic effects of a mitochondrion-targeted glutathione reductase inhibitor on restraining tumor cells

Renshuai Zhang [a,b,1], Na Xiao [c,1], Qi Xu [d], Qiuyu Gong [e], Fandong Kong [f,*], Hongfei Jiang [a,b,**]

[a] The Affiliated Hospital of Qingdao University, Qingdao University, Qingdao, 266071, China
[b] Cancer Institute, Qingdao University, Qingdao, 266071, China
[c] State Key Laboratory of Crop Biology, College of Agronomy, Shandong Agriculture University, Tai'an, Shandong, 271018, China
[d] School of Pharmaceutical Sciences, Laboratory of Immunology for Environment and Health, Shandong Analysis and Test Center, Qilu University of Technology (Shandong Academy of Sciences), Jinan, 250353, China
[e] Department of Thoracic Surgery, The First Affiliated Hospital of Xi'an Jiaotong University, Xi'an, 710061, China
[f] Key Laboratory of Chemistry and Engineering of Forest Products, State Ethnic Affairs Commission, Guangxi Key Laboratory of Chemistry and Engineering of Forest Products, Guangxi Collaborative Innovation Center for Chemistry and Engineering of Forest Products, School of Chemistry and Chemical Engineering, Guangxi Minzu University, Nanning, 530006, China

ARTICLE INFO

Keywords:
Mitochondria
Antitumor agents
Glutathione reductase
Metabolism
Redox homeostasis

ABSTRACT

Mitochondria has been identified as a target for tumor therapy. Agents preferentially concentrated in mitochondria may exert more potent antitumor effects by interfering with the normal function of mitochondria. Glutathione reductase (GR) in mitochondria is a crucial antioxidant enzyme to maintain mitochondrial function, and has been recognized as an important target for the development of anticancer drugs. Herein, we present a triphenylphosphonium-modified anticancer agent, **MT-1**, which can preferentially accumulate in mitochondria and bind to GR by covalent binding manner.

As a result, morphology and function of mitochondria were severely damaged, as well as cellular energy supply was severely impeded due to the simultaneously inhibition against mitochondrial respiration and glycolysis. Moreover, **MT-1** was found to bind to a completely new site of GR (C278) that has never considered as binding site of inhibitors before. This new binding mode led to the change of GR structure, which affected the stability of the transition state of the catalytic process, and finally led to the inhibition of GR activity. Thus, current study provided a potentially novel tumor therapeutic strategy by targeting novel sites of GR in mitochondrion.

1. Introduction

Mitochondria are considered as a powerhouse in eukaryotic cells, meanwhile, play critical roles in regulating cellular signaling pathways, cellular metabolism, and cell death [1]. Mitochondrial defects and dysfunctions are closely related to onset of many diseases, especially cancer [2]. Mitochondria show indispensable roles in tumor cellular survival, progression and metastasis, thus interrupting the metabolism of mitochondria can directly affect tumorigenesis and tumor progression [3]. Additionally, tumor cells show more negative mitochondrial membrane potentials (MMP) than normal cells ($\Delta\psi_m \approx -220$ mV *VS* -140 mV), which makes mitochondria to be an ideal target for the development of novel antitumor agents [4–6]. Some drugs have been reported to exert anti-cancer activity through targeting mitochondria and damage the production of mitochondrial intermediate metabolites that provided indeed building blocks for tumor anabolism (*e.g.*, CPI-613 in phase III and CB-839 in phase II) [7,8]. In addition, electrons leaking from mitochondria respiratory chain could be directly transferred to oxygen to generate reactive oxygen species (ROS), thus making mitochondria be one of the most significant sources of ROS, and may produce up to 90% of cellular ROS [9,10]. Levels of ROS is tightly associated with intracellular redox homeostasis that is the key for virtually all facets of tumor progression. Many agents targeting mitochondria have shown potent antitumor effects by affecting ROS levels and thus disrupting

* Corresponding author.
** Corresponding author. The Affiliated Hospital of Qingdao University, Qingdao University, Qingdao, 266071, China.
E-mail addresses: kongfandong0127@126.com (F. Kong), jianghongfei@qdu.edu.cn (H. Jiang).
[1] These authors contributed equally to this work.

https://doi.org/10.1016/j.ejmech.2022.115069
Received 1 November 2022; Received in revised form 23 December 2022; Accepted 27 December 2022
Available online 28 December 2022

redox homeostasis [11]. Considering mitochondria are major sites for ROS production, antioxidant enzymes in mitochondria, such as glutathione reductase (GR) and thioredoxin reductase (TrxR), are considered to be the first barrier against ROS [12,13]. Inhibition of these enzymes can disrupt the cellular defenses system against ROS, result in oxidative stress, affect mitochondrial function and further lead to cell death [14,15]. Therefore, targeting these antioxidant enzymes in mitochondria is considered to be an effective strategy for restraining cancer cells. Some metal complexes, such as those of Au, Ag, or Ru, have been found to show anticancer potency by inhibiting TrxR [16]. The development of antitumor drugs by targeting mitochondrial GR is still poorly reported.

Glutathione reductase (GR) is crucial in maintaining the intracellular redox homeostasis, and has become an attractive target for the development of anticancer drugs [17]. GR has also been shown to be overexpressed in human tumor tissues, and a high activity of the enzyme may be associated with tumor growth and resistance mechanisms against anticancer drugs [18]. Moreover, over a third of GR is localized in mitochondria [19,20]. Considering that mitochondria are an important source of ROS and target of oxidative damage, mitochondrial GR may play a more critical role in the cellular defense against oxidative damage. Many GR inhibitors have been found to possess anticancer potency, for example, FDA approved N, N-bis(2-chloroethyl)-nitrosourea (BCNU) showed strong GR inhibit activity, which has been proposed to contribute to both the therapeutic and toxic effects [21,22]. In addition, some chalcone analogues have demonstrated to target GR to exert anticancer activity, and the up-regulating of intracellular ROS is one of the characterized anticancer mechanisms [23–25]. However, these reported pharmacological activities are generally weak and ordinarily results in minor effectiveness. Accumulation of chalcones into mitochondria may result in stronger antitumor effect by inhibiting mitochondrial GR and upregulating ROS. However, so far, there are no reports on the use of chalcone analogues with mitochondrial targeting characteristics in antitumor research. Another focus is the effects of mitochondria and cell fate by mitochondrial GR inhibitors are largely unknown. Moreover, all of existing GR inhibitors bind in catalytic site, or a cavity located at the dimer interface, whether there are other effective binding sites remains unclear.

Herein we constructed a mitochondrion-targeted anticancer drug, **MT-1**, by decorating a novel chalcone with triphenylphosphine (TPP) unit. TPP has been widely used in the design of mitochondrion-targeted anticancer drugs for perturbing mitochondrial metabolism and redox homeostasis [16,26]. TPP modification greatly enhanced the inhibition activity against several tumor cells. The novel anticancer drug, **MT-1**, disturbed cellular redox homeostasis, caused tremendous damages to mitochondria, and induced mitophagy. In addition, **MT-1** impeded cellular energy supply through simultaneously inhibiting mitochondrial respiration and glycolysis. Thus, **MT-1** inhibited cancer cells *via* a multipronged manner (Fig. 1). Interestingly, **MT-1** bound to a completely new site (C278) of GR that has never been reported before, by a covalent binding manner. This new binding mode led to the change of GR structure, which affected the stability of the transition state of the catalytic process, and finally led to the inhibition of GR activity.

2. Results and discussion

2.1. Design and screening of *MT-1*

We first synthesized 14 novel chalcone analogues (CHD-1–14), and evaluated their cytotoxicity against a panel of human cancer cell lines, including HepG2, HeLa, A549, HCT116 and MCF-7 (Structures in Fig. 2A and Fig. S1, Synthetic route in Scheme S1, cytotoxicity in Fig. 2C and Table S1). Most of the compounds showed weak cytotoxicity against the five tumor cell lines. Considering the following two facts that up-regulating the generation of intracellular ROS was one of the characterized anticancer mechanisms of chalcones [23], meanwhile mitochondria was one of the most important sources of ROS [10], four TPP-modified chalcone analogues (**MT-1**–4) were synthesized with the aim of improving cytotoxicity by targeting mitochondria, disturbing mitochondria and further enhancing ROS. TPP modification significantly enhanced the cytotoxicity of chalcone analogues (CHD-1 *vs* **MT-1**, CHD-10 *vs* MT-2, CHD-3 *vs* MT-3, and CHD-8 *vs* MT-4), especially against HepG2 and HeLa cells (Fig. 2C and Table S1). Among these compounds, **MT-1** showed the optimal cytotoxicity against HeLa cells (Fig. 2C and S2). Thus, **MT-1** was selected as the target compound for the further study. Mitochondrial aggregation effect of **MT-1** was investigated by HPLC (Fig. S3). The result indicated that TPP modification caused more drug molecules to accumulate in mitochondria: drug molecules content in mitochondria of the **MT-1** treated cells was 2.75 times higher than that in the CHD-1 treated cells (Fig. 2B). In addition, ROS production was visualized using 2′,7′-dichlorofluorescin diacetate

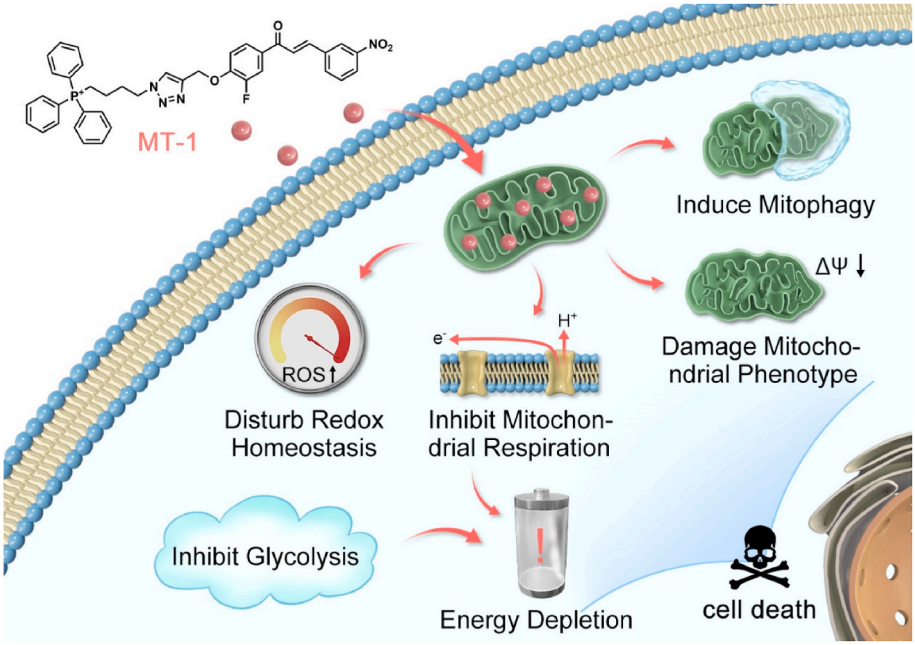

Fig. 1. Schematic illustration of **MT-1** inhibits cancer cells via a multipronged manner.

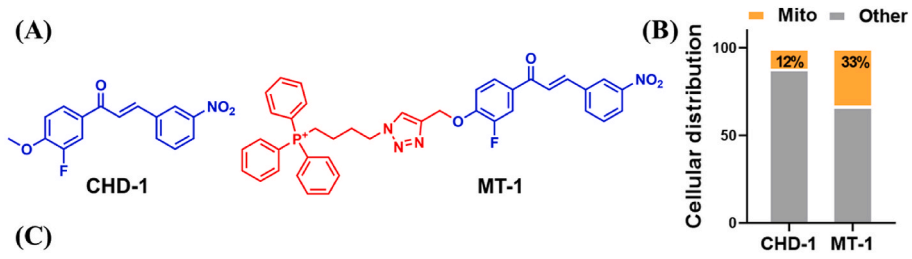

(C)

Compounds	HepG2	HeLa	A549	HCT116	MCF-7
MT-1	4.6 ± 0.1	2.4 ± 0.2	10.2 ± 0.8	8.2 ± 0.8	17.4 ± 0.2
CHD-1	> 50	> 50	> 100	> 50	> 100

Fig. 2. (A) Structures of CHD-1 and **MT-1**. (B) Distribution of drug molecules in mitochondria after treating HeLa cells with CHD-1 or **MT-1** for 6 h. (C) IC_{50} values (μM) of CHD-1 and **MT-1** for different cancer cell lines at 48 h. Data are shown as mean: standard deviation (S.D.; n = 3).

(DCFDA), a cell permeable fluorescent dye that was rapidly oxidized to a fluorescent molecule 2′,7′-dichlorodihydrofluorescein by intracellular ROS [27]. **MT-1** treatment increased cellular ROS production, implied a clear interference in redox homeostasis (Fig. S4). These results preliminarily confirmed the rationality of the compound design. Next, the effects of **MT-1** on HeLa cells were investigated in detail.

2.2. *MT-1 damaged mitochondrial morphology*

Mitochondria are indispensable subcellular organelles, and changes of mitochondrial morphology can affect the fate of cells [28]. The effect of **MT-1** on mitochondrial morphology in HeLa cells was investigated by transmission electron microscopy (TEM). Normal mitochondria showed clear cristae. While preincubation with **MT-1** at IC_{50} value for 48 h induced mitochondria to form multilayered vesicles, and treatment with 10 μM of **MT-1** led to the disappearance of cristae and the formation of vacuolar mitochondria (Fig. 3A), thus indicating that mitochondria were severely damaged. Immunofluorescence confirmed that **MT-1** induced increased expression of Mitofilin (IMMT), which was defined as a mitochondria-shaping protein in controlling and maintaining mitochondrial cristae structure (Fig. 3B) [29]. Thus, it provided a mechanism that **MT-1** damaged mitochondrial morphology.

2.3. *MT-1 impaired mitochondrial membrane potential*

MMP is a key parameter for evaluating mitochondrial function, which can reflect the damage of mitochondria [30]. The MMP of **MT-1** treated HeLa cells was detected using lipophilic cationic probe 5,5′,6,6′-tetrachloro-1,1′,3,3′-tetraethylbenzimidazolcarbocyanine iodide (JC-1), and the uncoupler carbonyl cyanide 3-chlorophenyl hydrazone (CCCP) was used as reference. [31] JC-1 can aggregate to emit red fluorescence when MMP in normal level, while remains as monomers that emit green fluorescence when MMP is dissipated. **MT-1** treated HeLa cells emitted green fluorescence, indicating the dissipation of MMP (Fig. 4A). Flow cytometric analysis was also performed to identify quantitatively the MMP in HeLa cells, with CCCP as reference. The contour plots show that the fluorescence in Q1 for high MMP was shifted to Q4 for low MMP (Fig. 4B). The centers of contour plots moved from Q1 to Q4 in concentration dependent manner after treatment of **MT-1**, thus suggesting that **MT-1** has a strong ability to dissipate the MMP. The results also suggest that the mitochondrial membrane was impaired by **MT-1**.

2.4. *MT-1 induced mitophagy*

The increase of ROS level and mitochondrial damage may induce autophagy or mitophagy [32]. TEM image upon treatment with **MT-1** in HeLa clearly displayed the formation of vacuoles of autophagosomes that was a marker of autophagy (Fig. S5). In addition, changes in the expression of autophagy-related proteins also provided direct evidence for autophagy [32]. Treatment with **MT-1** down-regulated expression of p62, and increased the ratio of lipidated LC3B-II to normal LC3B–I in a concentration dependent manner (Fig. 5A). Together, they confirmed the autophagic process induced by **MT-1**. Mitophagy was evaluated using confocal laser scanning microscopy (CLSM) and TEM. The encapsulation of mitochondria in lysosomes is an indicator of mitophagy [32]. The confocal images clearly displayed the colocalization of mitochondria and lysosomes in **MT-1** treated Caov3 cells, whereas no overlap

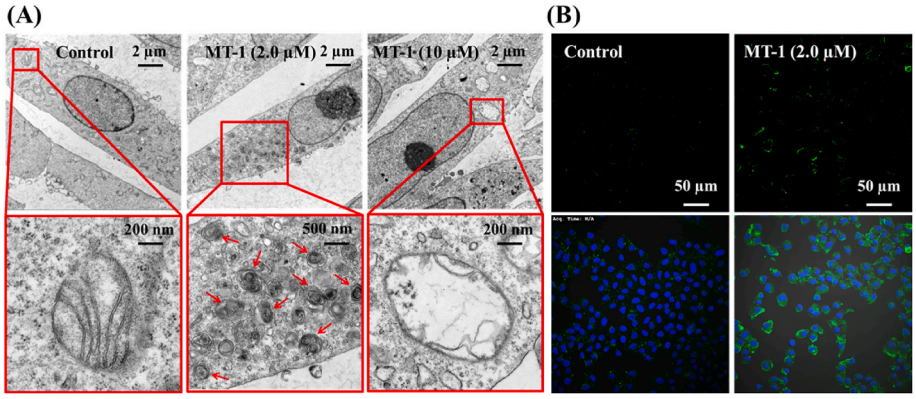

Fig. 3. (A) TEM images indicating the alterations of mitochondrial morphology in **MT-1** treated HeLa cells. (B) Confocal fluorescent images of IMMT in HeLa cells after incubation with **MT-1**, and staining with DAPI.

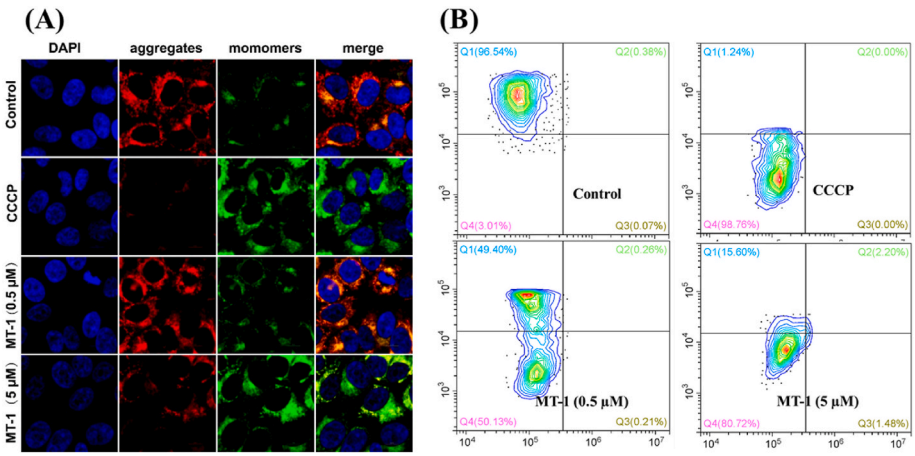

Fig. 4. Fluorescence microscopy images (A) and flow cytometry quantification (B) of JC-1-labeled HeLa cells treated with **MT-1** or CDDP for 24 h.

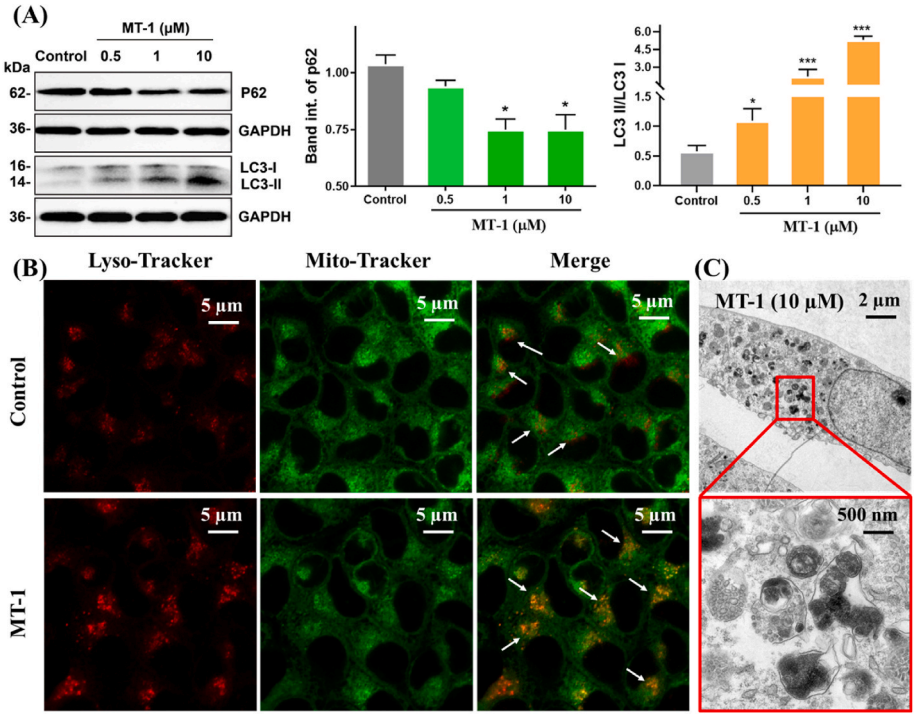

Fig. 5. (A) Immunoblotting of LC3 and p62 in HeLa cells treated with **MT-1** for 24 h and corresponding quantification of the p62 expression and LC3-II to LC3-I ratio. $^{*}P < 0.05$, $^{***}P < 0.001$. (B) Confocal fluorescent images showed colocalization of lysosomes and mitochondria in HeLa cells. HeLa cells were stained with LysoTracker® Red and MitoTracker® Green. (C) Representative TEM images of HeLa cells treated with **MT-1** for 48 h, emphasizing the region of mitophagy.

was observed for the control (Fig. 5B). In addition, TEM showed that mitochondria were capped in the vacuoles, thus indicating that they were removed from cells through autophagosomes (Fig. 5C). These results indicate that **MT-1** could induce mitophagy.

2.5. RNA-seq analysis

To determine the in-depth cytotoxic mechanisms of **MT-1**, whole genome RNA-seq was performed on HeLa cells treated with **MT-1**, with CHD-1 as a reference. The transcription of 17553 genes were examined. Among those genes, 309 genes were exclusively transcribed in the cells treated with CHD-1; 879 genes were exclusively transcribed in the **MT-1** treated cells (Fig. 6A). Compared with the control group, 783 genes were upregulated (red dots) and 790 genes were downregulated (green dots) in the CHD-1 group (Fig. 6B); however, 2484 genes were upregulated and 1744 genes were downregulated in the **MT-1** group (Fig. 6C). Compared with CHD-1 treated cells, 2454 genes were upregulated and 1758 genes were downregulated in **MT-1** treated cells (Fig. 6D). Specifically, autophagy-related genes such as MAP1LC3B [33], WIPI1 [34], and GADD45A [35] were found upregulated (Fig. 6E and F), which was consistent with previous studies. The protein-protein interaction was further depicted in Fig. S6, and autophagy-related genes were marked separately. Overall, RNA-seq analysis provided a comprehensive understanding of the changes in transcriptome and the alterations in autophagy pathways.

2.6. Metabolic analysis: mitochondrial respiration and glycolysis

The cellular ROS level, mitochondrial morphology, and MMP were closely related to mitochondrial respiration [12]. After confirming that **MT-1** can affect cellular redox balance, disrupt mitochondrial morphology and dissipate MMP, the oxygen consumption rate (OCR)

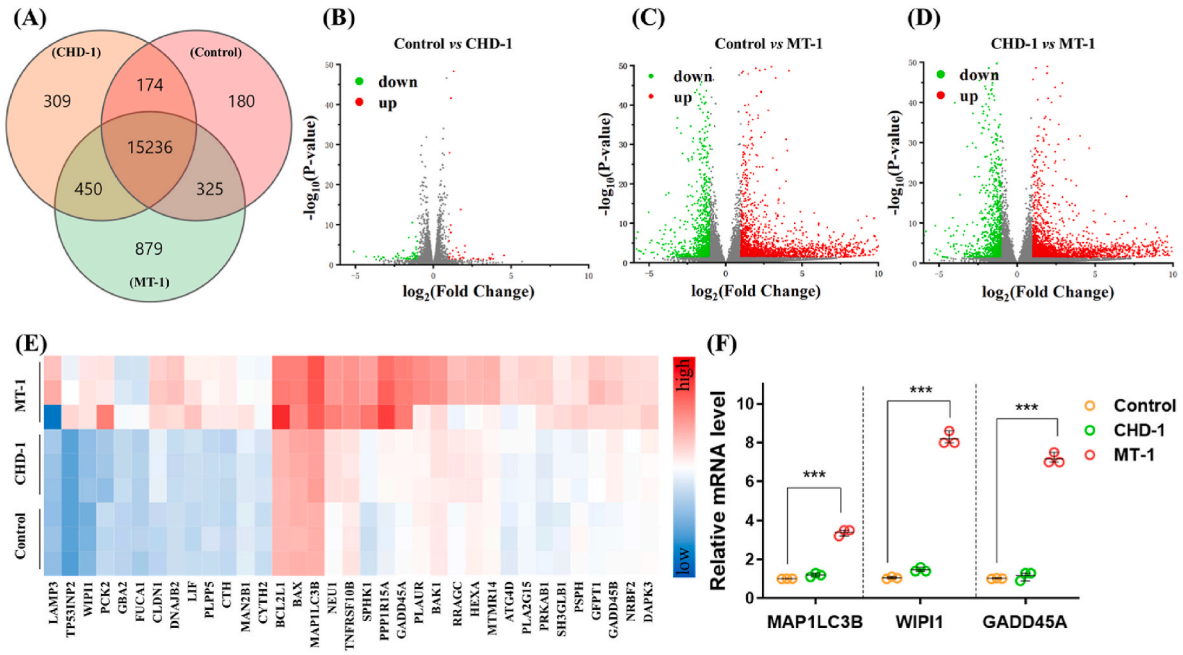

Fig. 6. Transcription analysis of HeLa cells treated with **MT-1** and CHD-1 by RNA-seq. (A) A Venn Diagram revealed the number of genes transcribed in each treatment group. (B–D) Volcano plots displayed the differentially expressed genes. (E) A heat map showing the transcription of genes of interest. (F) Quantitative analysis of the mRNA expression levels of autophagy-related genes. $^{***}P < 0.001$.

indicated mitochondrial respiration in **MT-1** treated HeLa cells was evaluated by a Seahorse XF bioenergetic system (Fig. 7). The OCR of mitochondria significantly decreased after treatment with **MT-1**, which indicated that **MT-1** can inhibit the mitochondrial respiration (Fig. 7A). Furthermore, the key energetic parameters reflecting the mitochondrial respiration functions were quantitatively assessed, including basal respiration, ATP production, and proton leak respectively (Fig. 7B). The result indicated that **MT-1** significantly repressed both basal respiration and ATP production capacity. In addition, proton leakage across the mitochondrial inner membrane can reduce the MMP, thus slightly increased proton leakage further confirmed the dissipation of MMP in **MT-1** treated HeLa cells, which was consistent with the result showed in Fig. 3. Similar results for OCR were also found in the HepG2 cells (Fig. S7A).

Metabolically flexible cancer cells can obtain ATP through switching path from mitochondrial respiration to aerobic glycolysis [3]. Simultaneous inhibition of both mitochondrial respiration and glycolysis can limit cell energy acquisition in a maximum extent. Therefore, we determined the effect of **MT-1** on aerobic glycolysis through testing the extracellular acidification rate (ECAR) in HeLa cells. As shown in Fig. 7C, basal ECAR was dramatically decreased by **MT-1**, indicating that **MT-1** can inhibit the glycolysis. Similar results were also found in

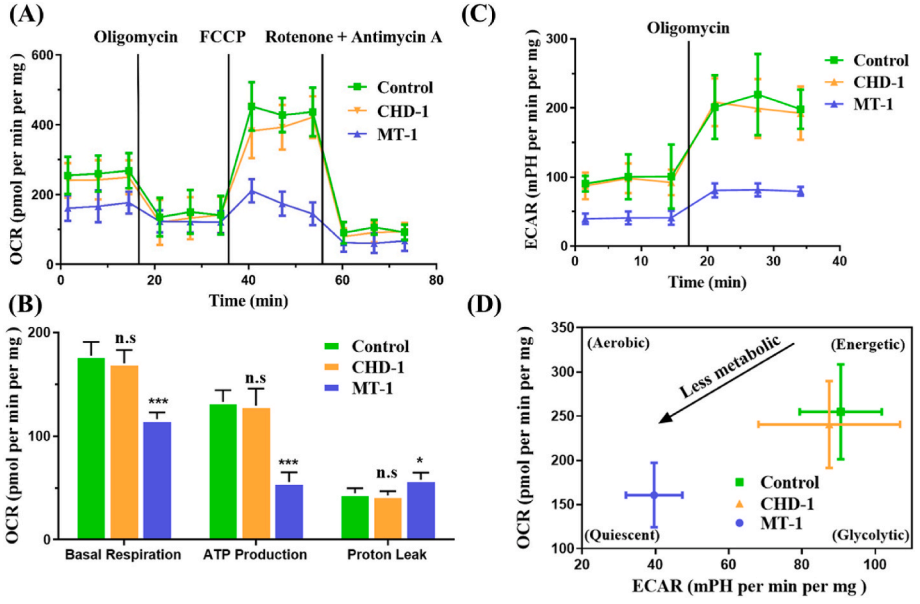

Fig. 7. (A) Kinetic profiles of OCR in HeLa cells after treatment with 2.0 μM **MT-1** for 24 h, with CHD-1 (2.0 μM) as reference. (B) Quantification of basal respiration, ATP production, and spare respiratory capacity from the kinetic profiles of OCR. n.s. not significant, $^{*}P < 0.05$, $^{***}P < 0.001$. (C) HeLa cells were measured by the mitochondrial stress kit to determine ECAR (**MT-1**: 2.0 μM; CHD-1: 2.0 μM). (D) Indices of metabolism as calculated from the OCR and ECAR profiles of HeLa cells.

the HepG2 cells (Fig. S7B), which further confirmed the suppression of glycolytic capacity by **MT-1**. The OCR versus ECAR profile indicated the contribution of two major pathways to energy production, and provided a more comprehensive understanding of bioenergetics [36]. As shown in Fig. 7D and S7C, **MT-1** induced dramatic decreases in both OCR and ECAR, thus indicating that mitochondria respiration and glycolysis were reduced simultaneously to give a hypometabolic state. Blocking of flexible metabolic adaption suggested that **MT-1** has the characteristics of inhibiting the metabolic heterogeneity of tumors, thus representing a more attractive strategy for chemotherapy.

2.7. Target identification of *MT-1*

The increase of cellular ROS levels was usually accompanied by a decrease in reduced glutathione, whereas **MT-1** significantly increased the ROS (Fig. S4) but did not cause the decrease of GSH levels in HeLa cells, which was demonstrated by GSH determination using a commercially available kit (Fig. S8A) and confocal imaging using a thiol-tracker, Thiol-tracker™ Violet (Fig. 8A and B). However, it was worth noted that a 2- to 10-fold increase of oxidized glutathione (GSSG) was observed in **MT-1** treated cells depending on the concentrations (Fig. S8B). Thus, intracellular GSH/GSSG ratio was significantly decreased to be in the range of 192/1–19/1 depending on concentration (Fig. 8C). Previous studies have shown that inhibition of GR can cause accumulation of GSSG and decrease the GSH/GSSG ratio [37,38]. GR was a key intracellular enzyme system for maintaining redox homeostasis, and its inhibition usually leads to increase of ROS levels, which was consistent with our previous experimental results (Fig. S4). Therefore, we evaluated the effects of **MT-1** on the purified GR activity. The activity of purified GR was dramatically inhibited by **MT-1** ($IC_{50} = 0.59$ μM), which was more potent than positive control BCNU, a commonly used GR inhibitor in research (Fig. 9A) [39]. In addition, CHD-1 had no inhibitory effect on purified GR. Furthermore, the effects of **MT-1** on total cellular and mitochondrial GR were also evaluated in HeLa cells. As shown in Fig. 9B, **MT-1** significantly reduced the activity of mitochondrial and cellular GR by 50% and 20%, respectively. Moreover, the expression of GR in HeLa cells was knocked out in order to investigate the influence of GR on the MT-1-mediated inhibition of cell viability. Western blot showed that the expression of GR was significantly down-regulated through CRISPR/Cas9-mediated genome editing (Fig. S9A). Then HeLa cells with GR knockout were treated with MT-1 for 48 h, and the cell viability was assayed. Results indicate that HeLa cells with GR knockout was less sensitive to the inhibitory effect of MT-1 with significant difference at 10 μM (Fig. S9B), implying the effect of MT-1 on HeLa cell viability was mainly dependent on GR.

Mass spectrometric was used to understand the mechanism of action of GR and **MT-1** [40]. The results indicated that **MT-1** covalently bind to Cys278 (C278) which was located in a completely new cavity, distinct from the known binding sites (the catalytic site and a cavity at the dimer interface) of the previously reported inhibitors (Fig. 9C) [41]. On the contrary, no covalent binding of CHD-1 to GR was detected (data not shown), which was consistent with our previous experimental results (Fig. 9A). C278 was located in a cavity far from (more than 20 Å) the catalytic site (containing C102 and C107), thus how **MT-1** binding to C278 to exert its inhibitory activity was worth exploring (Fig. S10). The catalytic mechanism of GR has been investigated for many decades, which involved electron transference between NADPH, FAD and the cysteine residue (C102 and C107) located in catalytic site [17]. Tyr241 (Y241) was highly conserved residue directly involved in catalysis activity of GR, and also was proposed to act as a spring in forcing the nicotinamide into the flavin (Fig. S10) [42]. The phenol ring of Y241 can form π-π overlap with the nicotinamide ring of NADPH and isoalloxazine ring of FAD in the catalytic process (Fig. S11A), which may play a crucial role in stabilizing the EH_2-NADPH complex, a stable equilibrium mixture of two electron reduced species. Even the slight movement of Y241 may affect the binding of NADPH and its interaction with FAD, thus interfering with the electron transfer among them and further affecting the catalytic activity of GR [42]. The binding site of **MT-1** (C278) was closer to Y241 than the catalytic site, and Y241 may be the bridge for **MT-1** to exert its inhibitory effect. This hypothesis was supported by the molecular dynamics (MD) simulation study of GR with **MT-1**. As shown in Fig. 9D, the unsaturated ketone structure of **MT-1** formed a covalent bond with C278 of GR through Michael addition reaction, as well as Y241 interacted with the benzene ring of chalcone structure through π-π overlap. Furthermore, results from MD simulations also showed that binding of **MT-1** had significant impact on the orientation of Y241, which was different from the previously reported conformations (Fig. 9E). This change of Y241 orientation significant

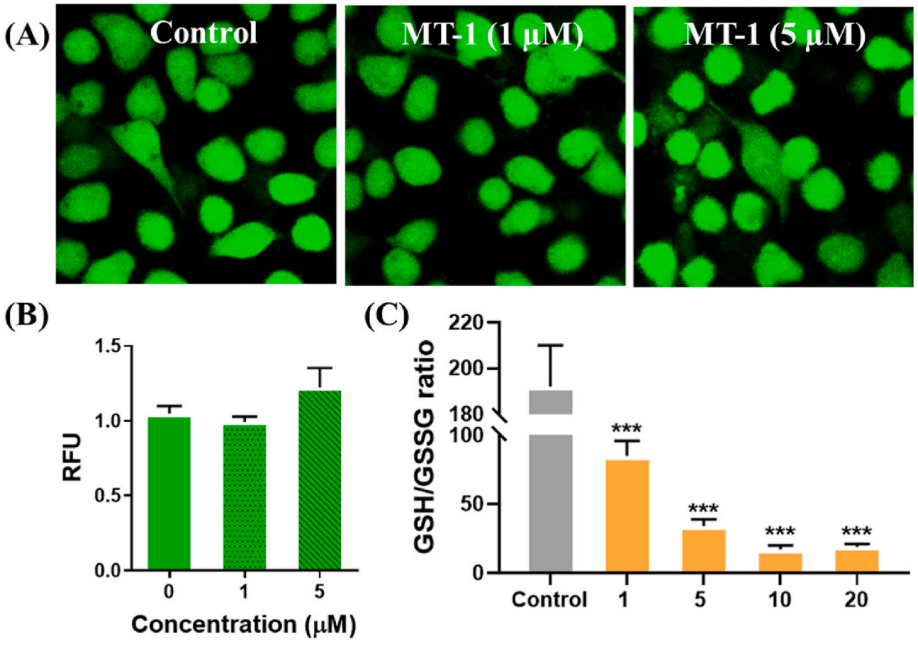

Fig. 8. Intracellular thiol-tracker fluorescence (A) and quantification (B) in HeLa cells incubated with required concentration of **MT-1** for 6 h. (C) The changes of the intracellular GSH/GSSG ratios in HeLa cells treated with **MT-1**. ***$P < 0.001$.

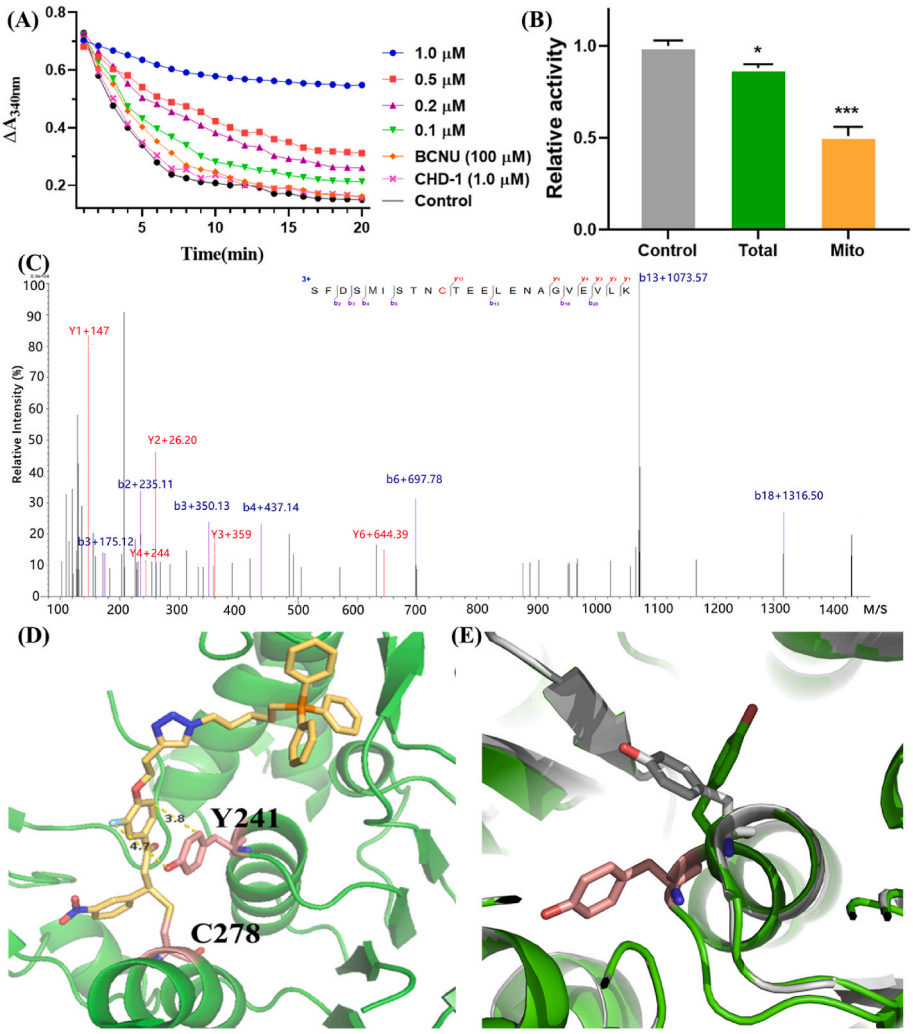

Fig. 9. Inhibition of the activity of purified GR by **MT-1** (A), and quantification of mitochondrial and total GR activity in HeLa cells treated with **MT-1** (B). (C) Mass spectrum of peptide *SFDSMISTNCTEELENAGVEVLK* containing C278 of GR treated with **MT-1**. (D) Covalently binding mode of the **MT-1** to GR (PDB: 2GH5). (E) Image of the conformational of Y241 in GR without NADPH binding (green, PDB: 2GH5), with NADPH binding (grey, PDB: 1GRB), and after MD simulation (orange).

disrupted the π-π overlap between Y241 and NADPH and FAD, which was confirmed by the following molecular docking study between **MT-1** modified GR with NADPH and FAD (Fig. S11B). Moreover, the binding of **MT-1** directly affected the stability of GR through RMSD investigation (Fig. S12). Thus, the results from MD and molecular docking study provided a possible explanation for the inhibition of GR activity by **MT-1**.

3. Conclusion

Currently, mitochondria have been promising targets for the development of novel anticancer agents, and targeting key enzymes within mitochondria has become one of the most important antitumor strategies. One of the characteristic mechanisms of chalcone antitumor was the up-regulation of ROS, which was closely related to mitochondria. In this study, a series of chalcone analogues were synthesized for screening antitumor agents. Thereafter, to enhance antitumor activity, TPP-decorated chalcone analogues were synthesized for targeting mitochondria and breaking redox homeostasis. Among these molecules, **MT-1** with the best antitumor activity was screened out on a panel of human cancer cell lines. **MT-1** preferentially accumulated in mitochondria and significantly increased intracellular ROS levels. In addition, **MT-1** could effectively break mitochondrial morphology and MMP, and induced mitophagy. A genome-wide analysis *via* RNA-seq was employed to provide a comprehensive understanding of the changes in transcriptome, showed that the genes involved autophagy pathways were significantly affected by **MT-1** treatment (q-value <0.05). Furthermore, **MT-1** inhibited mitochondrial respiration and glycolysis simultaneously, thus making cancer cells into a hypometabolic state and starving them to death. By measuring the level of GSH and the ratio change of GSH/GSSG, we inferred and further verified that GR was the target of **MT-1**. **MT-1** could not only effectively inhibit purified GR, but also significantly reduce the cellular and mitochondrial GR activity. HeLa cell-based assay with knock out GR expression verified that the effect of **MT-1** was dependent on GR expression. Mass spectrometric analysis showed that **MT-1** covalently bound to C278 of GR. MD simulation and molecular docking studies indicated that **MT-1** affected the conformation of Y241, interfered with the binding of NADPH, and broke the interaction between Y241, FAD and NADPH, which further disrupted the electron transport during GR catalysis and thus inhibited GR activity. This study highlighted the pleiotropic effects of a TPP-decorated chalcone analogue on the mitochondria and cancer cell fate through targeting mitochondrial GR, and proposed a novel binding site for GR covalent inhibitors, thereby offering a promising strategy for chemotherapy.

Author contributions

Renshuai Zhang designed the experiments and analyzed the results. Na Xiao designed the experiments. Qi Xu performed cell cultures and activity screening. Qiuyu Gong performed the flow cytometry experiments. Hongfei Jiang designed and supervised the experiments. Renshuai Zhang and Fandong Kong wrote the original draft of the manuscript. Hongfei Jiang and Na Xiao reviewed and edited the text.

Declaration of competing interest

The authors declare that they have no known competing financial interests or personal relationships that could have appeared to influence the work reported in this paper.

Data availability

Data will be made available on request.

Acknowledgements

We thank Shanghai Bioprofile Technology Co., Ltd. for technical support in mass spectroscopy. We are grateful to the Natural Science Foundation of Shandong Province (ZR2021QH212, ZR2020QC081); the Science and Technology Support Plan for Youth Innovation of Colleges and Universities of Shandong Province of China (20190164); Science, Education, and Industry Integration Technology Innovation Project (2022PX013); Guangxi Natural Science Foundation under Grant (2021GXNSFBA075036) for financial support.

Appendix A. Supplementary data

Supplementary data to this article can be found online at https://doi.org/10.1016/j.ejmech.2022.115069.

References

[1] Ph Willems, R. Rossignol, Ce Dieteren, Mp Murphy, Wj Koopman, et al., Redox homeostasis and mitochondrial dynamics, Cell Metabol. (22) (2015) 207–218.
[2] J. Nunnari, A. Suomalainen, et al., Mitochondria: in sickness and in health, Cell 148 (2012) 1145–1159.
[3] Pe Porporato, N. Filigheddu, Jmb Pedro, G. Kroemer, L. Galluzzi, et al., Mitochondrial metabolism and cancer, Cell Res. (28) (2018) 265–280.
[4] Ra Smith, Cm Porteous, Am Gane, Mp Murphy, et al., Delivery of bioactive molecules to mitochondria in vivo, Proc. Natl. Acad. Sci. U. S. A. 100 (2003) 5407–5412.
[5] Ga Vitiello, Bd Medina, S. Zeng, Tg Bowler, Jq Zhang, Jk Loo, Nj Param, M. Liu, Aj Moral, Jn Zhao, F. Rossi, Cr Antonescu, Vp Balachandran, Jr Cross, Rp Dematteo, et al., Mitochondrial inhibition augments the efficacy of imatinib by resetting the metabolic phenotype of gastrointestinal stromal tumor, Clin. Cancer Res. (24) (2018) 972–984.
[6] Hardev Singh, Divya Sareen, Jiyamary George, Vineet Bhardwaj, Saehee Rha, Sukjoong Lee, Sheetal Sharma, Amit Sharma, Jongseung Kim, et al., Mitochondria targeted fluorogenic theranostic agents for cancer therapy, Coord. Chem. Rev. (452) (2022), 214283.
[7] Shawnd Stuart, Alexandra Schauble, Sunita Gupta, Adamd Kennedy, Brianr Keppler, Paulm Bingham, Zuzana Zachar, et al., A strategically designed small molecule attacks alpha-ketoglutarate dehydrogenase in tumor cells through a redox process, Cancer Metabol. (2) (2014) 4.
[8] Jj Harding, M. Telli, P. Munster, Mh Voss, Jr Infante, A. Demichele, M. Dunphy, M. H. Le, C. Molineaux, K. Orford, F. Parlati, Sh Whiting, Mk Bennett, Nm Tannir, F. Meric-Bernstam, et al., A phase i Dose-Escalation and expansion study of telaglenastat in patients with advanced or metastatic solid tumors, Clin. Cancer Res. (27) (2021) 4994–5003.
[9] Md Brand, C. Affourtit, Tc Esteves, K. Green, Aj Lambert, S. Miwa, Jl Pakay, N. Parker, et al., Mitochondrial superoxide: production, biological effects, and activation of uncoupling proteins, Free Radic. Biol. Med. 37 (2004) 755–767.
[10] Ajbrandm Lambert, et al., Reactive oxygen species production by mitochondria, Methods Mol. Biol. 554 (2009) 165–181.
[11] H. Wang, J. Chang, M. Shi, W. Pan, N. Li, B. Tang, et al., A Dual-Targeted organic photothermal agent for enhanced photothermal therapy, Angew Chem. Int. Ed. Engl. 58 (2019) 1057–1061.
[12] Paola Venditti, Lisa Di Stefano, Sergio Di Meo, et al., Mitochondrial metabolism of reactive oxygen species, Mitochondrion (13) (2013) 71–82.
[13] Simrans Sabharwal, Pault Schumacker, et al., Mitochondrial ROS in cancer: initiators, amplifiers or an Achilles' heel? Nat. Rev. Cancer 14 (2014) 709–721.
[14] Junmin Zhang, Xinming Li, Xiao Han, Ruijuan Liu, Jianguo Fang, et al., Targeting the thioredoxin system for cancer therapy, Trends Pharmacol. Sci. (38) (2017) 794–808.
[15] Z. Zhu, S. Du, Y. Du, J. Ren, G. Ying, Z. Yan, et al., Glutathione reductase mediates drug resistance in glioblastoma cells by regulating redox homeostasis, J. Neurochem. 144 (2018) 93–104.
[16] Kun Wang, Chengcheng Zhu, Yafeng He, Zhenqin Zhang, Zhou Wen, Nafees Muhammad, Yan Guo, Xiaoyong Wang, Zijian Guo, et al., Restraining cancer cells by dual metabolic inhibition with a Mitochondrion-Targeted Platinum (II) complex, Angew. Chem. Int. Ed. (58) (2019) 4638–4643.
[17] Holger Bauer, Karin Fritz-Wolf, Andreas Winzer, Sebastian Kühner, Susan Little, Vanessa Yardley, Hervé Vezin, Palfey Bruce, Rheiner Schirmer, Elisabeth Davioud-Charvet, et al., A fluoro analogue of the menadione derivative 6-[2'-(3'-Methyl)-1',4'-naphthoquinolyl]hexanoic acid is a suicide substrate of glutathione reductase. Crystal structure of the alkylated human enzyme, J. Am. Chem. Soc. 128 (2006) 10784–10794.
[18] Jg Muller, Us Bucheler, K. Kayser, Rh Schirmer, D. Werner, Rl Krauth-Siegel, et al., Glutathione reductase in human and murine lung tumors: high levels of mRNA and enzymatic activity, Cell. Mol. Biol. (Paris, Fr., Print) 39 (1993) 389–396.
[19] As Mikosha, Aia Mestechkina, et al., Subcellular distribution of glutathione reductase and sulfhydryl groups in adrenal tissue, Biull Eksp Biol. Med. 73 (1972) 44–46.
[20] S. Ahmad, Ca Pritsos, Sm Bowen, Cr Heisler, Gj Blomquist, Rs Pardini, et al., Antioxidant enzymes of larvae of the cabbage looper moth, Trichoplusia ni: subcellular distribution and activities of superoxide dismutase, catalase and glutathione reductase, Free Radic. Res. Commun. (4) (1988) 403.
[21] Nina Doroshenko, Petro Doroshenko, et al., The glutathione reductase inhibitor carmustine induces an influx of Ca2+ in PC12 cells, Eur. J. Pharmacol. (497) (2004) 17–24.
[22] Gabrielil Parrilha, Karinaso Ferraz, Josanea Lessa, Kelynavakoski de Oliveira, Bernardol Rodrigues, Jonasp Ramos, Elainem Souza-Fagundes, Ingo Ott, Heloisa Beraldo, et al., Metal complexes with 2-acetylpyridine-N(4)-orthochloro-phenylthiosemicarbazone: cytotoxicity and effect on the enzymatic activity of thioredoxin reductase and glutathione reductase, Eur. J. Med. Chem. (84) (2014) 537–544.
[23] Lh Wang, Hh Li, M. Li, S. Wang, Xr Jiang, Y. Li, Ping Gf, Q. Cao, X. Liu, Wh Fang, Gl Chen, Jy Yang, Cf Wu, et al., SL4, a chalcone-based compound, induces apoptosis in human cancer cells by activation of the ROS/MAPK signalling pathway, Cell Prolif (48) (2015) 718–728.
[24] Chunlin Zhuang, Wen Zhang, Chunquan Sheng, Wannian Zhang, Chengguo Xing, Zhenyuan Miao, et al., Chalcone: a privileged structure in medicinal chemistry, Chem. Rev. 117 (2017) 7762–7810.
[25] Kai Zhang, Er-bin Yang, Wen-ying Tang, Kimping Wong, Peter Mack, et al., Inhibition of glutathione reductase by plant polyphenols, Biochem. Pharmacol. (54) (1997) 1047–1053.
[26] Suxing Jin, Yigang Hao, Zhenzhu Zhu, Nafees Muhammad, Zhenqin Zhang, Kun Wang, Yan Guo, Zijian Guo, Xiaoyong Wang, et al., Impact of Mitochondrion-Targeting group on the reactivity and cytostatic pathway of Platinum(IV) complexes, Inorg. Chem. (57) (2018) 11135–11145.
[27] Minsuk Shim, Younan Xia, et al., A reactive oxygen species (ROS)-Responsive polymer for safe, efficient, and targeted gene delivery in cancer cells, Angew. Chem. Int. Ed. (52) (2013) 6926–6929.
[28] Douglasc Wallace, et al., Mitochondria and cancer, Nat. Rev. Cancer (12) (2012) 685–698.
[29] Y. Feng, Nb Madungwe, Jc Bopassa, et al., Mitochondrial inner membrane protein, Mic60/mitofilin in mammalian organ protection, J. Cell. Physiol. (234) (2019) 3383–3393.
[30] Lb Chen, et al., Mitochondrial membrane potential in living cells, Annu. Rev. Cell Biol. 4 (1988) 155–181.
[31] Abaccaranicontrimkalashnikova Cossarizza, et al., A new method for the cytofluorometric analysis of mitochondrial membrane potential using the J-aggregate forming lipophilic cation 5,5′,6,6′-Tetrachloro-1,1′,3,3′-tetraethylbenzimidazolcarbocyanine iodide (JC-1), Biochem. Biophys. Res. Commun. 197 (1993) 40–45.
[32] Danielj Klionsky, et al., Guidelines for the use and interpretation of assays for monitoring autophagy, Autophagy (8) (2012) 445–544.
[33] B. Swaminathan, H. Goikuria, R. Vega, A. Rodriguez-Antiguedad, Medinaa Lopez, Mdelm Freijo, K. Vandenbroeck, I. Alloza, et al., Autophagic marker MAP1LC3B expression levels are associated with carotid atherosclerosis symptomatology, PLoS One (9) (2014), e115176.
[34] Patrice Codogno, Maryam Mehrpour, Tassula Proikas-Cezanne, et al., Canonical and non-canonical autophagy: variations on a common theme of self-eating? Nat. Rev. Mol. Cell Biol. 13 (2011) 7–12.
[35] Mauro De Santi, Luca Galluzzi, Simone Lucarini, Mariafilomena Paoletti, Alessandra Fraternale, Andrea Duranti, Cinzia De Marco, Mirco Fanelli, Nadia Zaffaroni, Giorgio Brandi, Mauro Magnani, et al., The indole-3-carbinol cyclic tetrameric derivative CTet inhibits cell proliferation via overexpression of p21/CDKN1A in both estrogen receptor-positive and triple-negative breast cancer cell lines, Breast Cancer Res. 13 (2011) R33.
[36] Surinder Kumar, Morgan Jones, Qing Li, Davidb Lombard, et al., Assessment of cellular bioenergetics in mouse hematopoietic stem and primitive progenitor cells using the extracellular flux analyzer, JoVE (175) (2021), e63045.
[37] Yong Zhao, Teresa Seefeldt, Wei Chen, Laura Carlson, Stoebner Adam, Sarah Hanson, Foll Ryan, Duanep Matthees, Srinath Palakurthi, Xiangming Guan,

et al., Increase in thiol oxidative stress via glutathione reductase inhibition as a novel approach to enhance cancer sensitivity to X-ray irradiation, Free Radic. Biol. Med. (47) (2009) 176–183.

[38] Jiashu Xie, Ashley Potter, Wei Xie, Christophina Lynch, Teresa Seefeldt, et al., Evaluation of a dithiocarbamate derivative as a model of thiol oxidative stress in H9c2 rat cardiomyocytes, Free Radic. Biol. Med. (70) (2014) 214–222.

[39] Teresa Seefeldt, Chandradhar Dwivedi, Greg Peitz, Jocqueline Herman, Laura Carlson, Zhiling Zhang, Xiangming Guan, et al., 2-Acetylamino-3-[4-(2-acetylamino-2-carboxyethylsulfanylcarbonylamino)- phenylcarbamoylsulfanyl] propionic acid and its derivatives as a novel class of glutathione reductase inhibitors, J. Med. Chem. (48) (2005) 5224–5231.

[40] X. Li, M. Ni, X. Xu, W. Chen, et al., Characterisation of naturally occurring isothiocyanates as glutathione reductase inhibitors, J. Enzym. Inhib. Med. Chem. (35) (2020) 1773–1780.

[41] Gn Sarma, Sn Savvides, K. Becker, M. Schirmer, Rh Schirmer, Pa Karplus, et al., Glutathione reductase of the malarial parasite plasmodium falciparum: crystal structure and inhibitor development, J. Mol. Biol. (328) (2003) 893–907.

[42] Rl Krauth-Siegel, Ld Arscott, A. Schonleben-Janas, Rh Schirmer, Chjr Williams, et al., Role of active site tyrosine residues in catalysis by human glutathione reductase, Biochemistry 37 (1998) 13968–13977.